

# High-Pressure High-Enthalpy Test Facility

E. R. PUGH,\* R. M. PATRICK,\* AND A. M. SCHNEIDERMAN†

*Avco Everett Research Laboratory, Everett, Mass.*

The feasibility of using a magnetic annular arc as the accelerator for a high-pressure, high-enthalpy flow test facility is discussed. Simple design criteria based upon empirical relations obtained in experiments indicate that this type of accelerator would have advantages over the usual arc type heaters at stagnation pressures up to 100 atm. The advantage increases at higher flow enthalpies and correspondingly lower pressures. A pulsed prototype for such a facility operating for 1 msec has been constructed. It has demonstrated successful operation at pressures above atmospheric and, what is more important, that the accelerator operates as a pump in contrast to being only a heater with measured pressure rises of more than a factor of 4 across the accelerator.

## Nomenclature

$J$	= current density in accelerator
$B$	= magnetic field in accelerator
$V_0$	= voltage across accelerator when $B = 0$
$L$	= anode radius
$U_c$	= critical velocity
$V_A$	= effective voltage for heat transfer to anode
$I$	= total accelerator current
$\omega\tau$	= Hall parameter
$V$	= voltage across accelerator
$\dot{Q}_{\text{anode}}$	= total heat transfer to anode
$P$	= power into accelerator
$\dot{q}_{\text{max}}$	= maximum allowable heat transfer to anode per unit area
$p_0$	= stagnation pressure
$\rho$	= gas density at accelerator exit
$u$	= gas velocity at accelerator exit
$\dot{m}$	= mass flow per unit area
$n$	= number density
$M$	= mass of gas molecule
$a$	= speed of sound upstream of accelerator
$e/m$	= change to mass ratio for an electron
$\sigma v$	= velocity averaged collision cross section for electrons
$\alpha$	= proportionality constant between mass flux and magnetic field
$j_\theta$	= azimuthal current density in accelerator
$j_r$	= radial current density in accelerator
$\Delta p_r$	= change in magnetic pressure from cathode to anode
$\Delta p_z$	= change in magnetic pressure in axial direction due to $j_r$
$\mu_0$	= permeability of vacuum
$L_c$	= radius of current on cathode tip
$H$	= enthalpy
$RT_0$	= 34 Btu/lb = $85 \times 10^4 \text{ ft}^2/\text{sec}^2$

## I. Introduction

MODERN re-entry trajectories and high-speed flight have created the need for flow simulation facilities capable of higher and higher stagnation pressures and flow enthalpies. This, in turn, has led to interest in accelerators using  $J \times B$  forces capable of operating at high gas density and energy. The magnetic annular arc (MAARC) is a plasma accelerator initially developed for space propulsion. This work produced configurations of high efficiency in terms of converting electrical energy into gas flow energy. Since

high efficiency is the prime prerequisite for producing high power density flows, the authors have adapted this device for operation at these higher levels. Besides the practical interest in high density  $J \times B$  accelerators there are some fundamental advantages for basic research in working at high density where mean free paths are small. The viscous boundary layers are thin (high Reynolds number flows) so that continuum magnetohydrodynamics is applicable to the bulk flow, and the current carrying regions should not be controlled by wall effects. For example, much of the low-density data on similar accelerators has been complicated by important viscous effects so that the high-density results reported here represent the most convincing demonstration of azimuthal Hall currents increasing the stagnation pressure across the accelerator. Diagnostics can become easier at high density where measurements of pressure and velocity are straightforward. The literature on magnetoplasma-dynamic thrusters, which includes the MAARC, is extensive, and a recent review by Nerheim and Kelly<sup>1</sup> contains over one hundred references.

The next section consists of a description of the MAARC accelerator along with some intuitive ideas on why this particular geometry works as well as it does. Section III combines the empirical relations found for the accelerator parameters with some engineering constraints to estimate the performance limits of this type of accelerator. Section IV describes the experiments to evaluate these estimates, and the last section is a brief summary of the important results.

## II. MAARC Accelerator

The MAARC accelerator is shown schematically in Fig. 1. It consists of a coaxial pair of electrodes, the cathode in the center, and an anode which also serves as a nozzle. The discharge takes place off the cathode tip between the two coaxial electrodes. An electromagnet coil concentric with the accelerator produces a dipole-like magnetic field aligned with the accelerator axis. This is a simple configuration so that the region of maximum heat transfer (the area of the anode near the cathode tip) can be easily water-cooled. The insulator holding the cathode inside the anode can be well back from the gas discharge region, five or more anode diameters back being common. With this configuration the current must flow through the gas. There is no way it can "short out" through gas boundary layers or across insulator walls, in contrast to linear  $J \times B$  accelerators.

The magnetic field is essential for operation at high efficiencies. It prevents the electrons from crossing the annulus freely, thereby increasing the voltage across the accelerator

Received April 1, 1970; revision received July 31, 1970. Supported by Department of the Air Force, Air Force Office of Scientific Research, Office of Aerospace Research, Arlington, Va., under Contract No. AF49(638)-1483.

\* Principal Research Scientist.

† Principal Research Scientist. Member AIAA.

and reducing the importance of electrode drops. It also lowers the heat loss by lowering the thermal conduction to the walls resulting from electrons. The axial magnetic field has been shown to be important in stabilizing the discharge against spoking.<sup>2</sup> This magnetic field also creates Hall currents which flow azimuthally and interact with the applied axial magnetic field to produce inward forces, increasing the stagnation pressure on the centerline and making possible the large values of stagnation pressure needed for this facility. We will show in Section IV that a fraction of the large magnetic pressures that can be obtained with simple dipole-like magnetic fields can be converted into gas stagnation pressure. The high-stagnation pressures required are thus obtained using magnetic pressures rather than gas pressure. A complete theory for the operation of this type of accelerator is not available, but azimuthal currents interacting with the dipole magnetic field are important.

### III. Performance Estimates for High-Pressure, High-Enthalpy Test Facility

In contrast to the linear  $J \times B$  accelerator in which theory is simple and practice is extremely difficult, in the MAARC type of accelerator the practice is simple but the theory is complicated. To the properties of high-current gas discharges must be added a flow in which the defining parameters, Mach number, magnetic Reynolds number, and beta, the ratio of the gas pressure to the magnetic pressure, all go through one in the flow region of interest. The flow is three-dimensional, although the azimuthal derivatives should be zero, since the azimuthal component of velocity cannot be neglected. In fact, it is possible that, independent of the Hall effect, azimuthal currents will arise from a radial pressure balance between centrifugal forces due to the azimuthal velocity and a magnetic pressure gradient resulting from the interaction of these azimuthal currents with the predominantly axial magnetic field.<sup>3</sup> The azimuthal velocity itself is a result of the interaction of the applied radial current with this same axial magnetic field.

Much experimental data has been obtained using accelerators of this kind, and empirical relations have been found outlining the important accelerator parameters. The earliest studies on this type of accelerator were aimed at a small steady flow device operating at 10–100 kw power levels for use as a thruster for space propulsion.<sup>3–5</sup> This work produced the efficient accelerator configuration used in the present studies and led to two extensions into pulsed high-power applications. The first of these used the MAARC accelerator as the driver for a high-velocity shock tube<sup>6</sup> and the second of these applications used the MAARC accelerator to produce

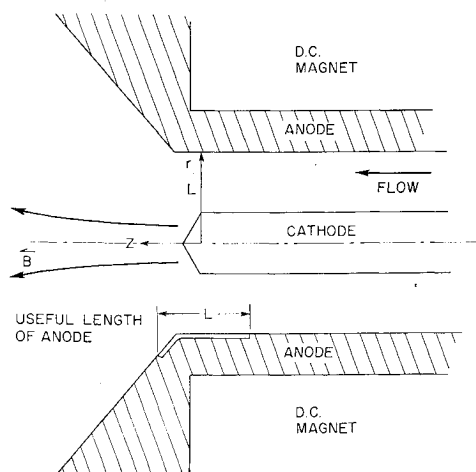


Fig. 1 Schematic diagram of MAARC accelerator.

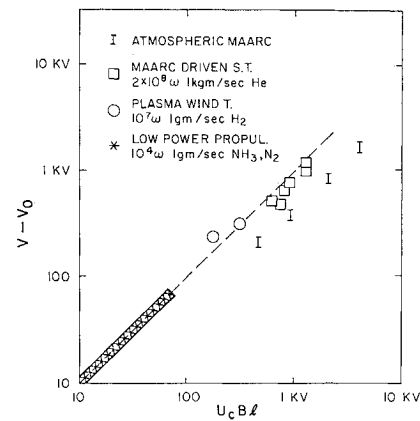


Fig. 2 Anode voltage as a function of  $U_c B L$ .

a high-velocity, low-density plasma for simulating the solar wind in a plasma wind tunnel.<sup>7</sup>

Data from these two more recent applications and the earlier studies of the d. c. experiments has been included with the results of the present studies (atmospheric MAARC) in Figs. 2 and 3, which show the empirical relations found for the accelerator voltage and anode heat transfer. The accelerator voltage is found to be equal to a small constant value  $V_0$  (which depends on the working gas and is approximately 25 v for nitrogen) plus a term which is proportional to the magnetic field and the distance  $L$  between the anode and cathode. The constant of proportionality has been found to be approximately the critical velocity as defined originally by Alfvén to be the velocity of a molecule such that its kinetic energy is equal to the energy necessary to ionize and dissociate it. The value of  $U_c$  for nitrogen is  $1.5 \times 10^4$  m/sec. Why the proportionality constant should be the critical velocity has never been satisfactorily explained. However, many attempts have been made and by now an extensive literature exists on this subject.<sup>8</sup> The data from the present experiments fall somewhat below the value  $U_c B L$ . This is thought to be due to the unsteady character of the present experiments, as will be discussed more in Section IV.

The heat transfer to the anode (Fig. 3) is proportional to the current in the accelerator with a proportionality constant  $V_A$  of approximately 25 v, similar to the value for  $V_0$ . The anode heat-transfer rate does not depend upon the magnetic field as long as the magnetic field is sufficiently high ( $\omega\tau > 1$ ) to maintain a uniform discharge.

Performance estimates using the MAARC accelerator can now be made for a high-pressure, high-enthalpy test facility. It has been found that the region over which the currents

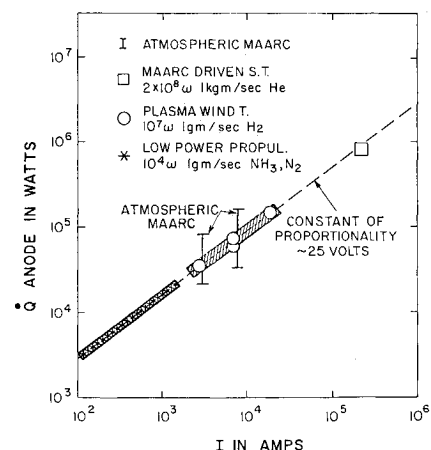


Fig. 3 Anode heat transfer vs current.

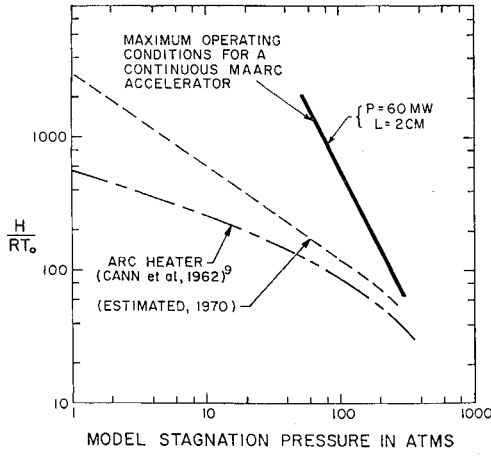


Fig. 4 Comparison of MAARC accelerator with arc heater for high-enthalpy high-pressure test facility.

flow to the anode is approximately equal to the anode-cathode space as shown in Fig. 1, and both will be denoted by  $L$  in the informal theory given here. These equations apply at the accelerator exit and thus provide an upper limit on the pressure measurements made further downstream. It is also assumed for simplicity that the Mach number at the accelerator exit is high so that the internal energy in the gas can be neglected:

$$V = V_0 + U_c BL \quad (1)$$

$$\dot{Q}_{\text{anode}} = V_A I \quad (2)$$

$$P = VI = (U_c BL)(\dot{q}_{\text{max}} 2\pi L^2 / V_A) \quad (3)$$

$$P/\pi L^2 < 2U_c BL / V_A \dot{q}_{\text{max}} \quad (4)$$

$$p_0 \cong \rho U^2 \quad (5)$$

$$P/\pi L^2 \cong \rho U U^2 / 2 \equiv \dot{m} U^2 / 2 \quad (6)$$

$$p_0 U \cong 2P/\pi L^2 \cong 4U_c BL / V_A \dot{q}_{\text{max}} \quad (7)$$

Equations (1) and (2) are the empirical relations just described. If the heat transfer to the anode is put equal to the maximum power that can be removed by water cooling,  $\dot{q}_{\text{max}}$  times the area of the current carrying region of the anode, then these two equations can be used to give the maximum power into the accelerator, and this is shown in Eq. (3). Dividing this by the frontal area of the accelerator gives Eq. (4), which relates the maximum power per unit area in the jet to the parameters  $U_c$  and  $V_A$  and the apparatus parameters, magnetic field  $B$ , size  $L$ , and maximum heat transfer  $\dot{q}_{\text{max}}$ .

With simple assumptions for  $p_0$  and  $P$  in terms of density  $\rho$  and velocity  $U$  (Eq. 5), the maximum power per unit area in the jet defines a maximum product of stagnation pressure  $p_0$  and velocity  $U$  that the jet may have, Eq. (6), and allows a comparison to be made between this type of accelerator and experiments with other test facilities using arc heaters. Such a comparison is made in Fig. 4. The estimated performance curve (1970) is based upon recent facility procurement specifications. Changing the mass flow through the accelerator gives different operating conditions on the maximum operating curve. As the mass flow is increased, the flow enthalpy decreases and the stagnation pressure increases. The curve shown in Fig. 4 used a magnetic field of 20 webers/m<sup>2</sup>, a maximum anode cooling rate of 10<sup>8</sup> w/m<sup>2</sup>,  $U_c = 1.5 \times 10^4$  m/sec, and  $V_A = 25$  v. The maximum  $p_0 U$  product is proportional to  $L$  so that larger devices have higher operating limits. This curve is drawn for an  $L$  of 2 cm giving an accelerator power level of 60 Mw. The maxi-

mum stagnation pressure is reached when the mass flow through the accelerator is so large that the accompanying gas density is too high and  $\omega\tau$  in the accelerator cannot be maintained above 1 for available magnetic field strengths. This can be helped somewhat by preheating the gas, giving higher flow velocities into the accelerator and correspondingly higher mass flows at the same density. In either case the mass flow through the accelerator for a given value of  $\omega\tau$  is proportional to the magnetic field strength,  $\dot{m} = \alpha B$ , so that  $p_{0\text{max}}$  is proportional to  $B$  [Eq. (7)]. The mass flow per unit area  $\dot{m} \leq nMa$ . So putting  $\omega\tau = 1$  gives a maximum value for  $\dot{m} < [(e/m)(Ma/\sigma v)]B = \alpha B$ . For  $N_2 M = 4.7 \times 10^{-26}$  kg,  $a = 3 \times 10^3$  m/s,  $e/m = 1.76 \times 10^{11}$  coul/kg, and  $\sigma v = 2.5 \times 10^{-14}$  M<sup>3</sup>/s corresponding to 0.2 ev electron. This makes  $\alpha = 10^2$  kg/wsec. For the 60 Mw size shown in Fig. 4 and  $\alpha = 10^2$  this maximum value is  $\cong 140$  atm. There is no known lower density limit for this accelerator. As has been previously mentioned, extremely high gas energies at low densities were obtained in the plasma wind tunnel application.

A small fraction of the magnetic pressure in the dipole field ( $B^2/2\mu_0 \cong 1600$  atm) must be converted through azimuthal currents via  $j_\theta \times B$  to flow stagnation pressure. This radial pressure rise can be evaluated in terms of the other accelerator parameters by defining an effective  $\omega\tau$ ,  $(\omega\tau)_{\text{eff}} \equiv j_\theta/j_r$ :

$$\Delta p_r \cong j_\theta BL = BL(\omega\tau)_{\text{eff}} \dot{q}_{\text{max}} / V_A \quad (8)$$

This pressure rise is also proportional to  $B$  but goes linearly with  $L$  as compared to  $L^{1/2}$  for the max stagnation pressure, so that larger devices require lower values of  $(\omega\tau)_{\text{eff}}$ . For the 60 Mw facility of Fig. 4,  $(\omega\tau)_{\text{eff}} \cong 8$  for  $p_0 = 140$  atm.

There is also the axial magnetic pressure due to the radial current  $j_r$  interacting with its own induced magnetic field  $B_\theta$ .

$$\Delta p_z = \frac{1}{\pi L^2} \int_{L_c}^L j_r B_\theta dV = \frac{\mu_0}{4\pi^2} \frac{I^2}{L^2} \ln \frac{L}{L_c} = \mu_0 \frac{\dot{q}_{\text{max}}^2}{V_A^2} L^2 \ln \frac{L}{L_c} \quad (9)$$

This average pressure rise depends logarithmically on the radius of the current leaving the cathode tip of radius  $L_c$ . For values of heat transfer  $\dot{q}_{\text{max}}$  allowable in continuous facilities this pressure is always negligible ( $\sim 10^{-1}$  atm for the 60 Mw facility of Fig. 4). Since this pressure increases as  $L^2$ , theoretically a size will be reached at which this term dominates; however, this occurs for  $L > 10M$ , a ridiculous size.

#### IV. Experiment

Figure 5 shows a schematic diagram of the atmospheric MAARC test facility prototype. It is a prototype in that it runs pulsed for a time of 1 msec. This means that the magnetic field coils, cathode and anode do not need to be water-cooled. However, in terms of mass flow, power level, and size it is similar to what a continuous test facility would be. Because the device was pulsed, a capacitor bank in the form of a transmission line was used that was capable of

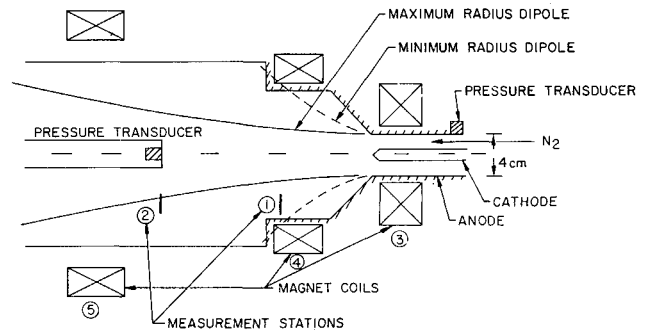


Fig. 5 Atmospheric MAARC test facility prototype.

delivering 10,000 amp for 1 msec at voltages up to 4000 v. A pulse transformer in series with the arc current applied a 60 kv pulse from cathode to anode to initiate the discharge. The gas supply was a tank truck and a regulator valve that provided a continuous flow of nitrogen at flow rates between 0.1 and 1 kg/sec. The energy for the magnetic fields was also obtained by a capacitor bank, this one having 120 kjoules at a voltage of 10 kv. The shape of the magnetic field was found to be important. If the magnetic field fringes too quickly, the accelerator current flows downstream along the annulus and crosses the field lines where they are weak. The large diameter coils downstream of the accelerator, coils 4 and 5 in Fig. 5, were used to trim the magnetic field from the main coil, 3, so that the effective coil radius (i.e., equivalent dipole size) could be varied from 7 cm for the small coil alone, to 50 cm when all three coils were activated. We found an effective radius of about 10 cm sufficient for preventing the currents from flowing downstream. Although the maximum field with coil 3 alone was 200 kgauss at the cathode tip, for the configuration giving an effective radius of 10 cm, the maximum field at the cathode tip was limited by the energy stored in the capacitor bank to 165 kgauss. In this configuration the magnetic field reached its maximum value in 5 msec. Two pressure probes are shown in Fig. 5, one upstream and one downstream mounted on a sting. Measurements were made at several radial positions at three axial locations: 9 cm, 19 cm, and 34 cm from the cathode tip. A typical current was 10 ka and, with a magnetic field strength of 165 kgauss, the accelerator voltage was 1600 v. This gives an input power of 16 Mw. The cathode was tungsten and the anode stainless steel. The heat transfer to the anode was not measured. However, the fact that the stainless steel anode was not marred implies that the total heat rejected to the anode was less than 5% of the total power (based on a transient heat conduction calculation).

Figure 6 is an oscillogram trace showing the pressure transducer signal. First the nitrogen is turned on and the required mass flow is set. The magnet bank is triggered and when it reaches its maximum, 5 msec later, the accelerator is turned on and lasts for 1 msec.

There is a time delay between the beginning of the accelerator current and the arrival of the pressure pulse at the probe. Measurements of this delay at the three axial positions indicate an average velocity of 600 m/sec. This represents an  $M = 2$  shock being driven into room temperature nitrogen. Since an  $M = 2$  shock at atmospheric pressure requires a driver pressure of 4.5 atm, this velocity is to be expected based on measured pressure increase. However, it is also clear that what is present is the starting process for the d. c. facility and not the final state. One msec is not long enough for the starting shock from the accelerator to sweep the air in front of it out of the way. There is no chance in these short times to measure high flow velocities even though the necessary pressure is present. However, the pressure increase across the accelerator can be measured.

Figure 7 shows measured pressure profiles at two axial positions. Notice that these downstream pressures measure as high as 4 times the upstream pressure. The upstream stagnation pressure shown in Fig. 7 was obtained by measuring the static pressure where the Mach number was low

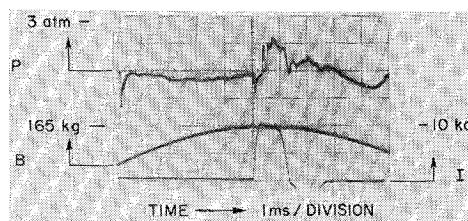


Fig. 6 Pressure signal vs time.

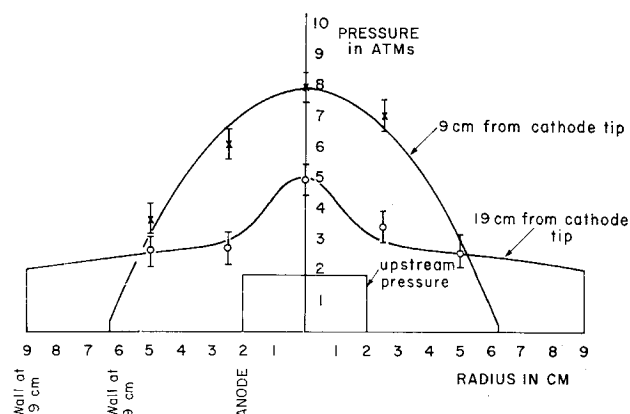


Fig. 7 Pressure vs time for two axial positions.

$M \sim 0.3$  and making the small corrections. The higher pressures measured on the centerline are a result of the azimuthal currents flowing in the gas interacting with the axial magnetic fields to create inward pressures. This effect is best seen by plotting centerline pressure vs magnetic field, Fig. 8. There is an apparent linear rise in centerline pressure with  $B$ . That this is an  $\omega r$  effect, or at least a  $B/\rho$  effect can be seen by varying the mass flow through the accelerator at constant magnetic field, Fig. 9. It is found that increasing the mass flow flattens the radial pressure distribution and actually decreases the centerline pressure.

The pressure 6 in. upstream of the accelerator was monitored and no increase in pressure at this location was found, even when the pressure downstream of the accelerator was four times higher. Thus, this pulsed device was able to act as a pump, which increased the pressure across the accelerator by a factor of 4.

The radiation from the discharge was examined with a photomultiplier and an optical system, such that a small portion of the discharge could be examined, and the time history of the light intensity was displayed on an oscilloscope. Although the discharge was quite "hashy," indicating temperature fluctuations in the discharge region, no periodic disturbances such as rotating spokes were found. The absence of spokes or periodic disturbances was further corroborated by placing two photomultipliers looking on opposite sides of the cathode  $180^\circ$  apart. No significant anticorrelation between the two signals was detected. The absolute magnitude of the light intensity is shown in Fig. 10. The intensity indicates that the gas is radiating as a blackbody at approximately  $7500^\circ\text{K}$ . This is in agreement with a value of  $H/RT_0 = 300$ , which would be expected from the measured input power and mass flow rate. There appears to be absorption at  $3900 \text{ \AA}$  probably as a result of the  $N_2^+(1-)$  bands of nitrogen. The fluctuations were not examined at small values of magnetic field and correspondingly low values of  $H/RT_0$  ( $H/RT_0 = 60$ ). There were no indications that this data was different from the higher enthalpy data even though the equilibrium conductivity in the gas would not be

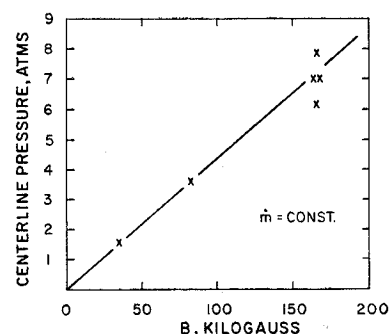


Fig. 8. Center line pressure vs magnetic field.

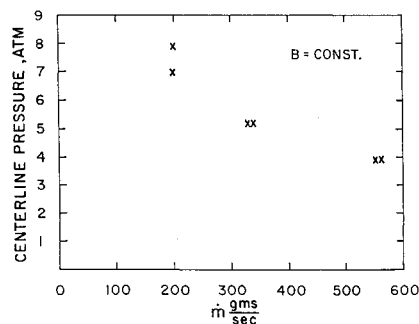


Fig. 9 Center line pressure vs mass flow.

expected to carry the current, and either nonequilibrium electron temperature or spatial nonuniformity would be expected.

The power input to the accelerator has gone into heating the slowly flowing gas. If the accelerator were on for a long time, the massive air ahead of the accelerator when it is turned on would be swept out of the way, and the gas velocity would rise until it was determined by the available stagnation pressure. It is thought that the accelerator operating in this unchoked high-velocity regime would have given the expected voltage  $U_c BL$ , and not the lower value measured in this experiment and shown in Fig. 2. This lower voltage means that the power into the accelerator is only 16 Mw as compared to the 60 Mw used in the theoretical calculations. However, more important for comparing experiment with the theory on Fig. 4 is the fact that high Mach number operation was not achieved as a result of the short test time. The theory assumes all the energy in the gas is in kinetic energy and this is not the case in the low Mach number operation achieved. Whether the gas velocity and accelerator voltage would rise given enough time is not known and will need d. c. experiments to determine.

## V. Summary

The feasibility of using a magnetic annular arc as the accelerator for a high-pressure, high-enthalpy flow test facility has been investigated. Simple design criteria, based upon empirical relations obtained in experiment indicate that this type of accelerator would have advantages over the usual arc-type heaters at stagnation pressures up to 100 atm. At lower stagnation pressures and higher flow enthalpies the advantage of this type of accelerator is indeed large (Fig. 4). A pulsed prototype for such a facility operating for 1 msec has been constructed. It has demonstrated successful operation at pressures above atmospheric and, more important, that the accelerator operates as a pump in contrast to being only a heater with measured pressure rises of more than a factor of 4 across the accelerator.

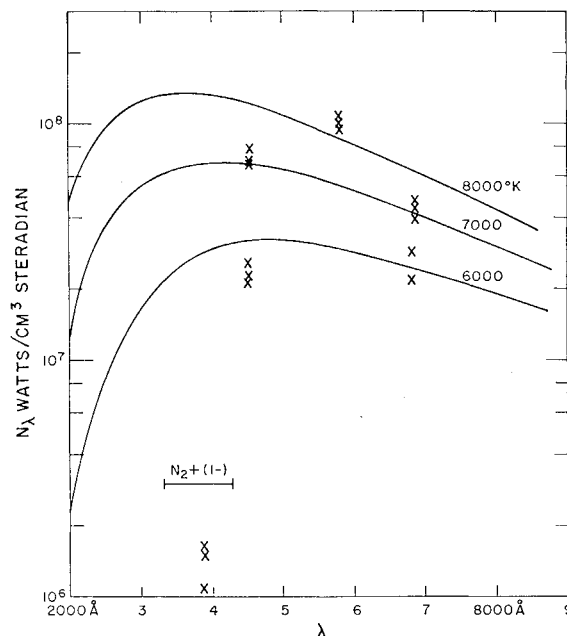


Fig. 10 Light intensity vs wave length.

## References

- 1 Nerheim, N. M. and Kelly, A. J., "A Critical Review of the Magnetoplasmadynamic (MPD) Thrustor for Space Applications," TR 32-1196, Feb. 1968, Jet Propulsion Lab., California Institute of Technology, Pasadena, Calif.
- 2 Cochran, R. A., "Experimental Investigation of the Occurrence and Behavior of Rotating Current Spokes in MPD Arcs," Ph.D. thesis, Jan. 1970, M.I.T., Cambridge, Mass.
- 3 Powers, W. E. and Patrick, R. M., "A Magnetic Annular Arc," *The Physics of Fluids*, Vol. 5, Oct. 1962, pp. 1196-1206.
- 4 Patrick, R. M. and Schneiderman, A. M., "Performance Characteristics of a Magnetic Annular Arc," *AIAA Journal*, Vol. 4, No. 2, Feb. 1966, pp. 283-290.
- 5 Schneiderman, A. M. and Patrick, R. M., "Optimization of the Thermal Efficiency of the Magnetic Annular Arc," *AIAA Journal*, Vol. 4, No. 10, Oct. 1966, pp. 1836-1838.
- 6 Schneiderman, A. M., Pugh, E. R., and Patrick, R. M., "A Magnetic Annular Arc Driven Shock Tube," *The Physics of Fluids*, Vol. 11, 1968, p. 278.
- 7 Pugh, E. and Patrick, R. M., "Plasma Wind Tunnel Studies of Collision-Free Flows and Shocks," *The Physics of Fluids*, Vol. 10, Dec. 1967, p. 2579.
- 8 Patrick, R. M. and Schneiderman, A., "Reply by Authors to R. Giovannella," *AIAA Journal*, Vol. 5, No. 8, Aug. 1967, p. 1531.
- 9 Cann, G. L. and Buhler, R. D., "A Survey and Prediction of the Performance Capability of Coaxial Arc Heaters," *Arc Heaters and MHD Accelerators for Aerodynamic Purposes*, AGARDograph 84, 1964.